

The magnetic ordering in the mixed valence compound $\beta\text{-Na}_{0.33}\text{V}_2\text{O}_5$

A. N. Vasil'ev

M. V. Lomonosov Moscow State University, 119899 Moscow, Russia

V. I. Marchenko, A. I. Smirnov, S. S. Sosin

P. L. Kapitza Institute for Physical Problems RAS, 117334 Moscow, Russia

H. Yamada, Y. Ueda

Institute for Solid State Physics, University of Tokyo, 7-22-1 Roppongi, Minato-ku, Tokyo 106, Japan
(November 13, 2018)

The low-temperature electron spin resonance (ESR) spectra and the static magnetization data obtained for the stoichiometric single crystals of $\beta\text{-Na}_{0.33}\text{V}_2\text{O}_5$ indicate that this quasi-one-dimensional mixed valence compound demonstrates at $T_N = 22$ K the phase transition into the canted antiferromagnetically ordered state. The spontaneous magnetization of $3.4 \times 10^{-3} \mu_B$ per V^{4+} ion was found to be oriented along the two-fold b axis of the monoclinic structure, the vector of antiferromagnetism is aligned with the a axis and the Dzyaloshinsky vector is parallel to the c -axis. The experimental data were successfully described in the frame of the macroscopic spin dynamics and the following values for the macroscopic parameters of the spin system were obtained: the Dzyaloshinsky field $H_D = 6$ kOe, the energy gaps of two branches of the spin wave spectrum $\Delta_1 = 48$ GHz and $\Delta_2 = 24$ GHz.

PACS numbers: 76.50.+g, 75.50.Ee, 75.25.+z

I. INTRODUCTION

The quasi-one-dimensional mixed valence compound $\beta\text{-Na}_{0.33}\text{V}_2\text{O}_5$ exhibits various phase transitions of a considerable interest.¹⁻³ Below 230 K the $1 \times 2 \times 1$ crystal lattice superstructure appears, indicating probably the ordering of Na ions. At $T_c = 136$ K this one-dimensional conductor exhibits a metal-insulator phase transition of a charge ordering type and at $T = T_N = 22$ K the charge-ordered structure undergoes an antiferromagnetic phase transition.

This behavior is to be compared with that of the quasi-one-dimensional magnet $\alpha\text{-NaV}_2\text{O}_5$ in which the lattice, charge and spin subsystems transform simultaneously. The charge ordering in this related system causes the opening of the spin gap in the spectrum of magnetic excitations and the appearance of a nonmagnetic singlet state.⁴⁻⁶

The $\beta\text{-Na}_{0.33}\text{V}_2\text{O}_5$ has the monoclinic structure $\text{C}2/m$ (see Fig. 1) with the unit cell containing two $\text{NaV}_6\text{O}_{15}$ formula units. The sodium ions are located in the tunnels formed by a V-O framework. The Na^+ ions occupy only one of the two nearest-neighboring sites A in the ac -plane. The V-O framework consists of the three distinct kinds of double chains directed along the b -axis.^{7,8} The V1-sites have a six-fold octahedral coordination and form a zigzag chain of edge-sharing VO_6 octahedra. The V2-sites with a similar octahedral coordination form a two-leg ladder chain of corner-sharing VO_6 octahedra, and the V3-sites, having a five-fold square pyramidal coordination form a zigzag chain of edge-sharing VO_5 pyramids.

The absence of the Knight shift in NMR experiments on ^{23}Na nuclei⁹ shows that the outer s -shell electrons

of the Na-ions are transferred into the d -shells of V-ions. Therefore, the V-ions are in the mixed valence states V^{4+} and V^{5+} . The V^{4+} ions are in a magnetic $S = \frac{1}{2}$ state, while the V^{5+} ions with $S = 0$ are nonmagnetic. Basing on interatomic distances¹⁰ and on NMR measurements^{11,12} it was concluded that in the high temperature phase $T > T_c$ the donated electrons are situated at the V1 sites, with one half of these sites being V^{4+} . The recent NMR experiments on V-ions¹³ confirm the charge ordering nature of the transition at $T = T_c$ and reveal that the number of inequivalent V positions below T_c is increased. Two possible models of the charge ordering (zigzag and linear chains of V^{4+} ions) are proposed but the exact crystal structure in a low temperature phase is still unknown.

Hypothetical models of the magnetic structure with the localized electrons suggest that only one-sixth part of the V ions has the magnetic moments and the magnetic subsystem of $\beta\text{-Na}_{0.33}\text{V}_2\text{O}_5$ appears to be strongly diluted. Nevertheless, the transition to the long-range magnetically ordered state occurs at an appreciably high temperature $T_N = 22$ K. The aim of the present work was to study in details the magnetic ordering in $\beta\text{-Na}_{0.33}\text{V}_2\text{O}_5$ by means of magnetic resonance and static magnetization measurements.

II. EXPERIMENTAL

A. Samples and the experimental techniques

The single crystals of a stoichiometric $\beta\text{-Na}_{0.33}\text{V}_2\text{O}_5$ were grown by a self flux technique using NaV_3O_8 as a

flux. The crystals of a typical size $5 \times 0.5 \times 0.2 \text{ mm}^3$ were obtained by melting the mixture of one part of $\text{Na}_{0.33}\text{V}_2\text{O}_5$ powder and thirty parts (weight ratio) of NaV_3O_8 powder. The melting at 740°C and cooling down to 600°C with a rate of 0.5°C/h were performed in a vacuum. The flux was removed by diluted hydrochloric acid. The longest dimension of the rectangular sample was aligned with the b axis, the middle dimension was aligned with the c axis, and the shortest dimension, denoted below as a' was perpendicular to the (bc) -plane. The crystallographic a axis is directed at an angle of 18° with respect to a' axis in the $a'c$ plane. The static magnetization measurements were done by the Quantum Design SQUID magnetometer. The magnetic resonance measurements in the frequency range 18-80 GHz were performed by the transmission type microwave spectrometer. The sample was put into the rectangular resonator having a set of eigen-frequencies in this range.

The temperature dependencies of the magnetization of $\beta\text{-Na}_{0.33}\text{V}_2\text{O}_5$ sample measured along the a' , b and c axes at the magnetic field $H = 10 \text{ kOe}$ are shown in Fig. 2. The change of the slope on these curves at $T_c = 136 \text{ K}$ marks the metal-insulator transition associated with the charge redistribution between the vanadium sites. The sharp increase in magnetization is observed at $T = T_N$.

The field dependencies of magnetization measured along the a' , b and c axes at $T = 5 \text{ K}$ are shown in Fig. 3. The asymptotically linear behavior of the $M(H)$ dependencies indicate the existence of the antiferromagnetic ordering. The residual magnetization $M(H = 0)$ for $\mathbf{H} \parallel b$ (as well as the anisotropic anomaly on $M(T)$ curves at $T = T_N$) are the evidence of a canting of the antiferromagnetic sublattices. The nonlinear part of the $M(H)$ curve at $\mathbf{H} \parallel a'$ should result from a spin-reorientation process. The extrapolation of $M(H)$ to $H = 0$ at $\mathbf{H} \parallel b$ gives a finite value of the spontaneous magnetization with a weak ferromagnetic moment of about $3 \times 10^{-3} \mu_B$ per V^{4+} ion.

The ESR absorption lines of $\beta\text{-Na}_{0.33}\text{V}_2\text{O}_5$ obtained as the field dependencies of the signal transmitted through the resonator with the sample at various temperatures are shown in Fig. 4. In the paramagnetic state (at $T > T_N$) the ESR line is observed at a slightly larger field than the DPPH reference ($g = 2.0$). Below T_N the ESR line rapidly shifts to lower magnetic fields.

The evolution of the ESR absorption with the frequency at $T = 4.2 \text{ K}$ is illustrated in Fig. 5. Up to four resonant lines marked by letters A, B, C, D were present in the absorption at different frequencies and sample orientations. The C and D lines disappear above 10 K and could not be ascribed to the ordered state, while the A and B lines exist in the whole temperature range below T_N and thus, should be of an antiferromagnetic type.

The magnetic resonance data at $T = 4.2 \text{ K}$ are summarized in Figs. 6a,b,c, in which the frequencies of the resonant lines are plotted *vs* magnetic field oriented along the a' , b and c axes respectively. The spectrum of the magnetic resonance in the ordered phase appears to be

highly anisotropic. It consists of two branches with the gaps of 48 GHz and 24 GHz. The falling branch of the magnetic resonance spectrum at $\mathbf{H} \parallel a'$ and the drop-to-zero of its resonance frequency at $H = 6 \text{ kOe}$ clearly indicate the spin-reorientation process ended by a phase transition of the second kind. The characteristic feature of the field dependencies of the resonance frequencies at $\mathbf{H} \parallel a'$ and b is the nonzero slope of both branches. The smaller of these slopes reveals the existence of canting of sublattices.

III. DISCUSSION

The general form of the antiferromagnetic resonance spectra and the magnetization curves prove the appearance of the canted antiferromagnetic state in $\beta\text{-Na}_{0.33}\text{V}_2\text{O}_5$ below $T < T_N$. The detailed analysis given below will allow us to obtain its macroscopic parameters.

Using the phenomenological approach¹⁴ we calculated the field dependencies of the static magnetization and the resonance spectra of a canted antiferromagnet with two axes of anisotropy for the various orientations of the magnetic field. According to this approach the antiferromagnetic structure is considered to be collinear in the exchange approximation, and the effects resulting from relativistic interactions (the sublattices canting and the anisotropy) are taken into account as perturbations. At low temperature the Lagrange function of a mole of such an antiferromagnet may be represented in the form:

$$\mathcal{L} = \frac{\chi_\perp}{2\gamma^2}(\dot{\mathbf{l}} - \gamma[\mathbf{lH}])^2 - \frac{\chi_\perp}{\gamma}(\mathbf{d}, \dot{\mathbf{l}} - \gamma[\mathbf{lH}]) - U_a, \quad (1)$$

where \mathbf{l} is the unit vector of the order parameter, χ_\perp is the antiferromagnetic susceptibility, γ is the magnetomechanical ratio (suggested to be equal to that of a magnetic V ion $\gamma = g\mu_B/h$), \mathbf{d} is the Dzyaloshinsky vector giving rise to the spontaneous magnetization $\mathbf{M}_{sp} = \chi_\perp[\mathbf{d}\mathbf{l}]$, U_a is the potential energy of the relativistic anisotropy taken as the quadratic form in the vector \mathbf{l} components:

$$U_a = \frac{\beta_1}{2}(\mathbf{x}\mathbf{l})^2 + \frac{\beta_2}{2}(\mathbf{y}\mathbf{l})^2. \quad (2)$$

Here β_1, β_2 are positive constants of anisotropy, unit vectors \mathbf{x} and \mathbf{y} determine two orthogonal directions in the crystal. One of these two directions (corresponding to the largest coefficient β_i) should be the hard direction for the spin structure, the other one should be the middle direction, the third orthogonal unit vector \mathbf{z} will be an easy axis (the direction of the vector \mathbf{l} at $\mathbf{H} = \mathbf{0}$). The orientation of vectors \mathbf{x} , \mathbf{y} , \mathbf{z} and \mathbf{d} with respect to the crystal axes a , b and c is *a priori* not known, except for the condition that one of the vectors \mathbf{x} , \mathbf{y} or \mathbf{z} should be parallel to the two-fold axis b .

The total static magnetization of this system is:

$$\mathbf{M} = \frac{\partial \mathcal{L}}{\partial \mathbf{H}} = \chi_\perp(\mathbf{H} - \mathbf{l}(\mathbf{lH}) + [\mathbf{d}\mathbf{l}]). \quad (3)$$

The equilibrium value of the vector \mathbf{l} is determined by minimizing the potential energy of the system $\mathcal{P} = -\mathcal{L}(\dot{\mathbf{l}} = 0)$. The magnetic moment $M(H)$ measured in the experiment is the projection of \mathbf{M} onto \mathbf{H} .

The crystal symmetry requires the spontaneous moment \mathbf{M}_{sp} to be either parallel or perpendicular to the two-fold b axis. The static magnetization measurements confirm the first orientation. At the same time the extrapolation of $M(H)$ at $\mathbf{H} \parallel c$ to $H = 0$ gives no net magnetic moment. In accordance with formula (3) it means that the vector product $[\mathbf{d}\mathbf{l}]$ should be perpendicular to \mathbf{H} in high fields. The only possibility to satisfy this condition is to align vector \mathbf{d} with the c axis.

The easy direction \mathbf{z} of a canted antiferromagnet should be perpendicular to \mathbf{M}_{sp} and hence, lie in the ac plane. Thus, either \mathbf{x} or \mathbf{y} should be parallel to b axis. Taking this orientation for vector \mathbf{y} , we have also the vector \mathbf{x} in the ac plane. We shall denote the angle between the vectors \mathbf{d} and \mathbf{x} as α (see the inset to Fig. 3). This angle is not determined by the monoclinic symmetry and in principle may be arbitrary.

To describe the dynamical properties of the system one should find the variation of the Lagrange function (1) by \mathbf{l} :

$$\delta\mathcal{L} = \left(\frac{\partial\mathcal{L}}{\partial\mathbf{l}} - \frac{d}{dt} \frac{\partial\mathcal{L}}{\partial\dot{\mathbf{l}}} \right) \delta\mathbf{l}. \quad (4)$$

Taking $\delta\mathbf{l} = [\delta\theta\mathbf{l}]$, where $\delta\theta$ is the vector of a small rotation, we obtain the following system of nonlinear equations:

$$[\mathbf{l}, -\ddot{\mathbf{l}} + 2\gamma[\dot{\mathbf{l}}\mathbf{H}] + \gamma^2[\mathbf{H}[\mathbf{l}\mathbf{H}]] + \gamma^2[\mathbf{H}\mathbf{d}] - \Delta_1^2\mathbf{x}(\mathbf{x}\mathbf{l}) - \Delta_2^2\mathbf{y}(\mathbf{y}\mathbf{l})] = 0, \quad (5)$$

where $\Delta_{1,2}^2 = \gamma^2 \frac{\beta_{1,2}}{\chi_\perp}$ are two independent phenomenological parameters corresponding to two energy gaps of the spectrum. The linearized equations obtained from (5) by expanding \mathbf{l} in the vicinity of equilibrium give the resonance spectrum of the system.

When the vectors \mathbf{d} and \mathbf{z} are mutually perpendicular i.e. at $\alpha = 0$ the resonant frequencies may be calculated analytically for three basic orientations of the magnetic field.

1. $\mathbf{H} \parallel \mathbf{z}$: in this case the spin reorientation occurs under magnetic field. It is the continuous rotation of the vector \mathbf{l} in the plane containing easy and middle axes. Two intervals of the magnetic field should be considered separately.

- a) $H < H_c$: the equilibrium angle ψ between \mathbf{l} and \mathbf{z} is determined by the condition

$$\sin\psi = \frac{H_D H}{\Delta_j^2 / \gamma^2 - H^2}, \quad (6)$$

where $H_D = |\mathbf{d}|$, Δ_j is a smaller of the constants $\Delta_{1,2}$. The rotation terminates at

$H = H_c$ determined by the relation $\sin\psi = 1$, when \mathbf{l} becomes perpendicular to \mathbf{H} .

The resonance frequencies ω_1 and ω_2 are the roots of the biquadratic equation:

$$(\omega^2 + A)(\omega^2 + B) - 4\gamma^2 H^2 \cos^2\psi \omega^2 = 0, \quad (7)$$

where $A = \gamma^2(H^2 \cos^2\psi + H_D H \sin\psi) - \Delta_i^2 + \Delta_j^2 \sin^2\psi$,
 $B = (\gamma^2 H^2 - \Delta_j^2) \cos 2\psi + \gamma^2 H_D H \sin\psi$, Δ_i is the largest of $\Delta_{1,2}$.

- b) $H > H_c$:

$$\begin{aligned} \omega_1^2 &= \Delta_i^2 - \Delta_j^2 + \gamma^2 H H_D \\ \omega_2^2 &= \gamma^2 H(H + H_D) - \Delta_j^2. \end{aligned} \quad (8)$$

2. $\mathbf{H} \parallel \mathbf{x}$:

$$\begin{aligned} \omega_1^2 &= \gamma^2 H^2 + \Delta_1^2 \\ \omega_2^2 &= \Delta_2^2. \end{aligned} \quad (9)$$

3. $\mathbf{H} \parallel \mathbf{y}$:

$$\begin{aligned} \omega_1^2 &= \Delta_1^2 \pm \gamma^2 H H_D \\ \omega_2^2 &= \Delta_2^2 \pm \gamma^2 H(H + H_D). \end{aligned} \quad (10)$$

The signs \pm correspond to the domains of positive and negative directions of the spontaneous magnetization with respect to the magnetic field. On increasing the field the negative domain disappears and the corresponding resonance line disappears too according to our observations.

The resonance frequencies calculated by formulae (7-10) are represented in Figs. 6a,b,c by dashed lines. For an arbitrary value of α ($\alpha \neq 0$) the equilibrium orientation of \mathbf{l} in magnetic field was found numerically (for three orientations $\mathbf{H} \parallel a', b, c$) and then substituted to the expression for the magnetization and to the appropriate linearized equations of motion.

Finding the antiferromagnetic susceptibility $\chi_\perp \approx 3.2 \times 10^{-3}$ emu/mol V^{4+} from the slope of $M(H)$ curve at $\mathbf{H} \parallel c$ and varying the other four parameters α , H_D , Δ_1 and Δ_2 one can fit the magnetization curves and the resonance spectra for all three orientations. The best fit to experimental data was obtained for $\alpha = 18^\circ$, $\Delta_1 = 48$ GHz ($\beta_1 = 1.1 \times 10^{-2}$ K per V^{4+} ion), $\Delta_2 = 24$ GHz ($\beta_2 = 2.7 \times 10^{-3}$ K per V^{4+} ion) and $H_D = 6$ kOe. The results of this fitting are shown in Fig.3 and Fig.6 by solid lines. The determined value of $\alpha = 18^\circ$ means that the easy direction of the spin system \mathbf{z} is near the crystallographic axis a . It should be noted that the resonance spectrum at $H \parallel a'$ is very sensitive to the value of α due

to the effect of dynamic repulsion between two antiferromagnetic resonance branches.¹⁵ The intersection of the two branches may be observed at the exact orientation of the field along the z or y directions (it was observed at $\mathbf{H} \parallel \mathbf{y}$, see Fig. 6b). The "repulsion" is clearly seen in Fig. 6a at $\mathbf{H} \parallel \mathbf{a}'$ when the magnetic field appeared to be tilted with respect to z . The relation $\Delta_1 > \Delta_2$ indicates that \mathbf{x} is the hard axis and \mathbf{y} is the middle axis of the ordered spin structure. The mismatch between the observed and calculated resonance frequencies for the first branch in low fields at $\mathbf{H} \parallel \mathbf{b}$ remains unclear.

The magnetization is also described satisfactorily for $\mathbf{H} \parallel \mathbf{c}$ and for $\mathbf{H} \parallel \mathbf{b}$ (except for the small low field region associated with the poling). The agreement for the third orientation $\mathbf{H} \parallel \mathbf{a}'$ appears to be only qualitative, but still covers the most remarkable feature – the low field nonlinear part (mentioned in the Section 2) appearing due to the process of the continuous spin reorientation.

The above approach to the description of the uniform magnetic properties of a spin system is self-consistent and does not require any suggestions except that the exchange structure of the system is not strongly distorted by relativistic interactions. To evaluate the exchange integral from our data we will for simplicity neglect for the effect of zero point fluctuations¹⁶ on the susceptibility of quasi-one-dimensional system. In the molecular field approximation one can obtain the intrachain exchange integral $J = (g\mu_B)^2 N_A / 4k_B \chi_{\perp} \simeq 120$ K which corresponds to the molecular field $H_e = 1700$ kOe. The approximate evaluation for the Neel temperature of a quasi-one-dimensional antiferromagnet $T_N \sim \sqrt{JJ_{\perp}}$ gives the value for the interchain exchange interaction $J_{\perp} \sim 1$ K.

For anisotropy fields H_{A1} and H_{A2} corresponding to the values $\beta_{1,2}$ we have the following estimations: $H_{A1} = 340$ Oe, $H_{A2} = 85$ Oe. From the value of Dzyaloshinsky field $H_D = 6$ kOe we obtain that the spontaneous magnetization $M_{sp} = \chi_{\perp} H_D = 3.4 \times 10^{-3} \mu_B$ per V^{4+} ion which is in qualitative agreement with the data of Ref. 2.

IV. CONCLUSIONS

The magnetic resonance spectra and the magnetization curves obtained at low temperatures in the mixed valence charge ordered quasi-one-dimensional compound $\beta\text{-Na}_{0.33}\text{V}_2\text{O}_5$ confirm the transition into the canted antiferromagnetic state. The easy-direction of the spin system and the vector of the spontaneous magnetization are found to be aligned with the a axis and b axis correspondingly. The Dzyaloshinsky vector was found to be directed along c axis. The hard axis of the spin structure lies in the ac plane at an angle of 18° with respect to c axis, direction b is the middle axis of the spin anisotropy. The values of the intra and interchain exchange integrals as well as the anisotropy fields and the Dzyaloshinsky field are obtained.

V. ACKNOWLEDGMENTS

Authors thank H.Nojiri for cooperation in static magnetization measurements, L.A. Prozorova and V.D. Buchelnikov for valuable discussions. This work was supported by the Russian Fund for Basic Researches grants 00-02-17317 and 99-02-17828, INTAS grant 99-0155, NWO grant 047-008-012 and CRDF grant RP1-2097.

-
- ¹ R. P. Ozerov, G. A. Gol'der, G. S. Zhdanov, Sov. Phys.-Crystallogr. **2**, 211 (1957).
 - ² C. Schlenker, R. Buder, V.D.Nguyen, and J. Dumas, J. Appl. Phys. **50**, 1720 (1979).
 - ³ H. Yamada and Y. Ueda, J.Phys. Soc. Jpn. **68**, 2735 (1999).
 - ⁴ M. Isobe and Y. Ueda J. Phys. Soc. Jpn. **66**, 1178 (1996).
 - ⁵ Y. Fujii, H. Nakao, T. Yoshihama, M. Nishi, K. Nakajima, K. Kakurai, M. Isobe, Y. Ueda, H. Sawa, J. Phys. Soc. Jpn. **66**, 326 (1997).
 - ⁶ A. I. Smirnov, M. N. Popova, A. B. Sushkov, S. A. Golubchik, D. I. Khomskii, M. V. Mostovoy, A. N. Vasil'ev, M. Isobe and Y. Ueda, Phys. Rev. B **59**, 14546 (1999).
 - ⁷ A. D. Wadsley, Acta Crystallogr. **8**, 695 (1955).
 - ⁸ E. Deramond, J.-M. Savariault, and J.Galy, Acta Crystallogr. **C50**, 164 (1994).
 - ⁹ K. Maruyama and H. Nagasava, J. Phys. Soc. Jpn. **48**, 2159 (1980).
 - ¹⁰ J. B. Goodenough, J.Sol.St.Chem. **1**, 349 (1970).
 - ¹¹ M. Onoda, T. Takahashi and H. Nagasava, Phys. Stat. Sol. **B109**, 793 (1982).
 - ¹² M. Onoda, T. Takahashi and H. Nagasava, J. Phys. Soc. Jpn. **51**, 3868 (1982).
 - ¹³ M. Itoh, N. Akimoto, H. Yamada, M. Isobe, Y. Ueda, J. Phys. Soc. Jpn. **69** Suppl. B, 155 (2000).
 - ¹⁴ A. F. Andreev, V. I. Marchenko, Usp. Fiz. Nauk **130**, 39 (1980) [Sov.Phys.Usp. **23**, 21 (1980)].
 - ¹⁵ A. S. Borovik-Romanov, L. A. Prozorova, Pisma Zh. Eksp. Teor.Fiz. **4**, 57 (1966) [JETP Letters **4**, 39 (1966)].
 - ¹⁶ M. E. Zhitomirsky, I. A. Zaliznyak, Phys.Rev.B **53**, 3428 (1996).

Figure captions

- Fig. 1. The crystal structure of $\beta\text{-Na}_{0.33}\text{V}_2\text{O}_5$.
 Fig. 2. The temperature dependencies of the susceptibility M/H for three principal orientations of the magnetic field.
 Fig.3. The magnetization curves at $T = 5$ K
 Inset: The orientation of the Dzyaloshinsky vector \mathbf{d} , hard, middle and easy axes (see the text) with respect to crystallographic axes.
 Fig. 4. The temperature evolution of the ESR absorption line measured at the frequency $f = 24$ GHz ($\mathbf{H} \parallel \mathbf{b}$).

Fig. 5. The ESR lines at different frequencies at $T = 4.2$ K ($\mathbf{H} \parallel b$).

Fig. 6. The ESR spectra for three orientations of the magnetic field at $T = 4.2$ K. Symbols are the experimental data (closed ones on the panel b represent the low intensity absorption ascribed to "negative" domains). The dashed lines are drawn by formulae (7-10) with $\Delta_1 = 48$ GHz, $\Delta_2 = 24$ GHz and $H_D = 6$ kOe; solid lines are the result of theoretical calculations (see text) for "positive" domains, dashed-dotted lines are those for "negative" domains.

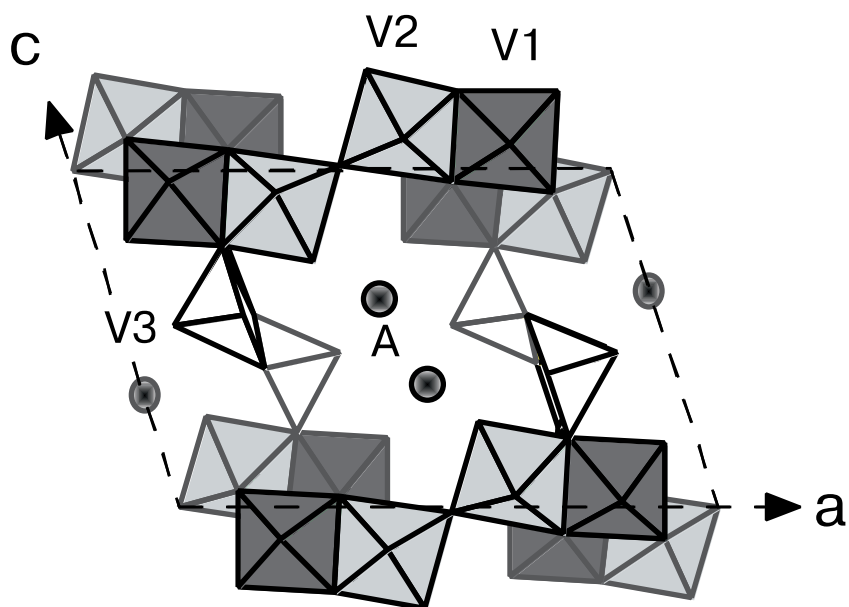


Fig. 1 Vasil'ev et.al.

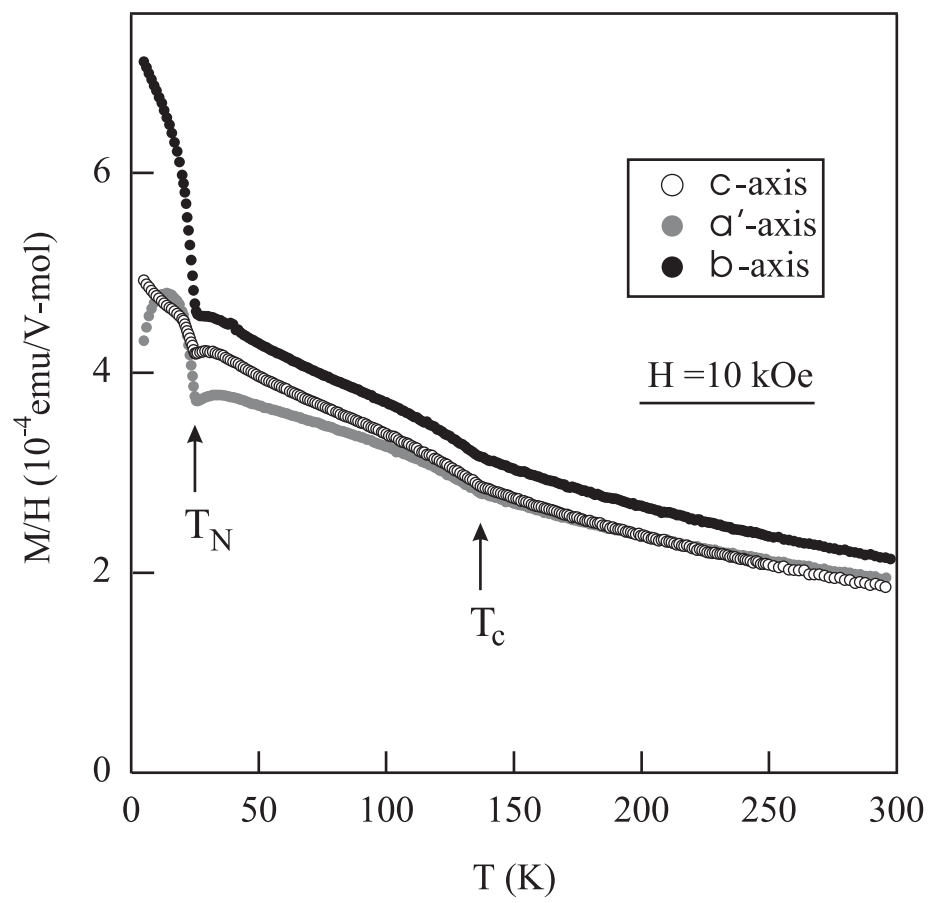


Fig. 2 Vasil'ev et.al.

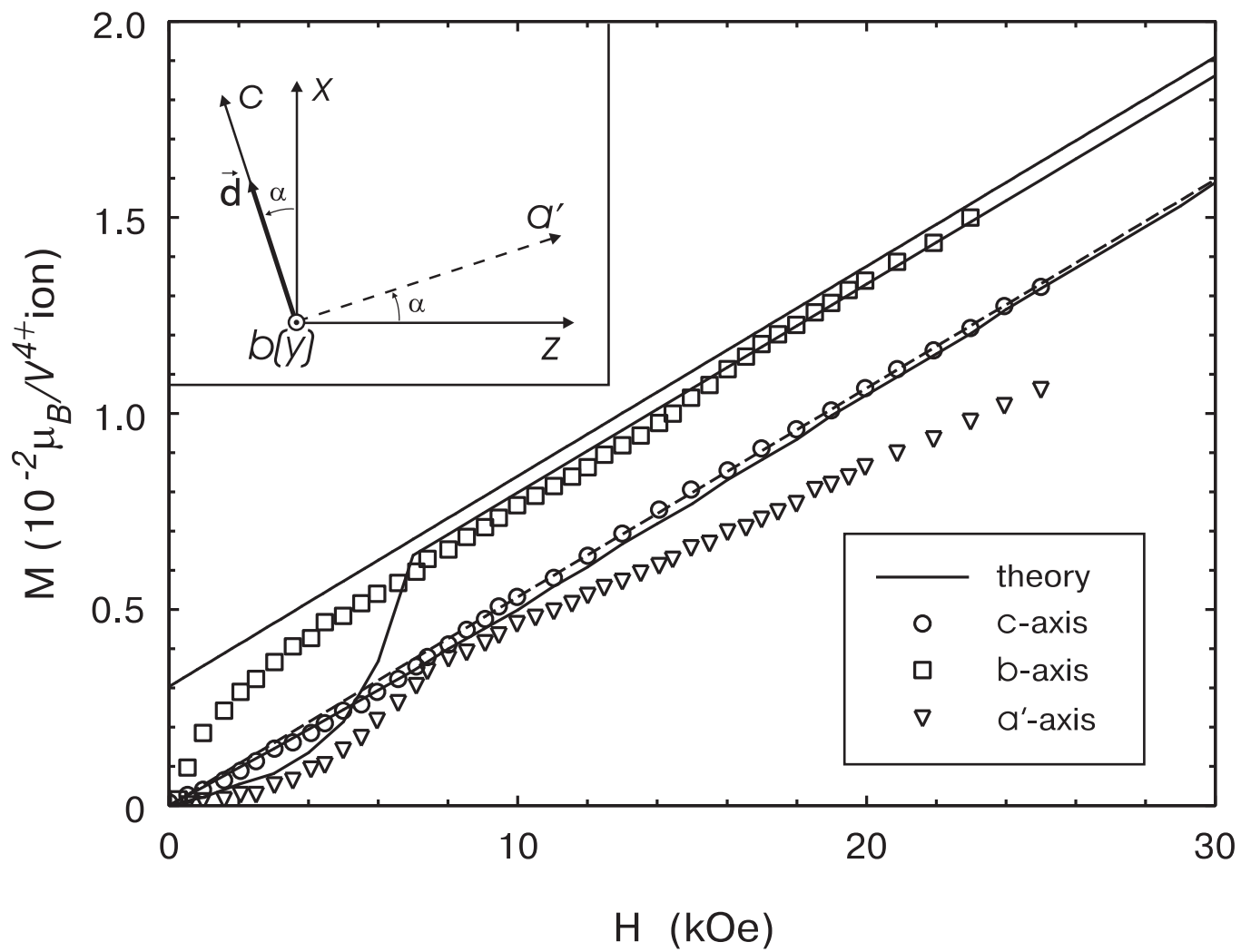


Fig. 3, Vasil'ev et.al.

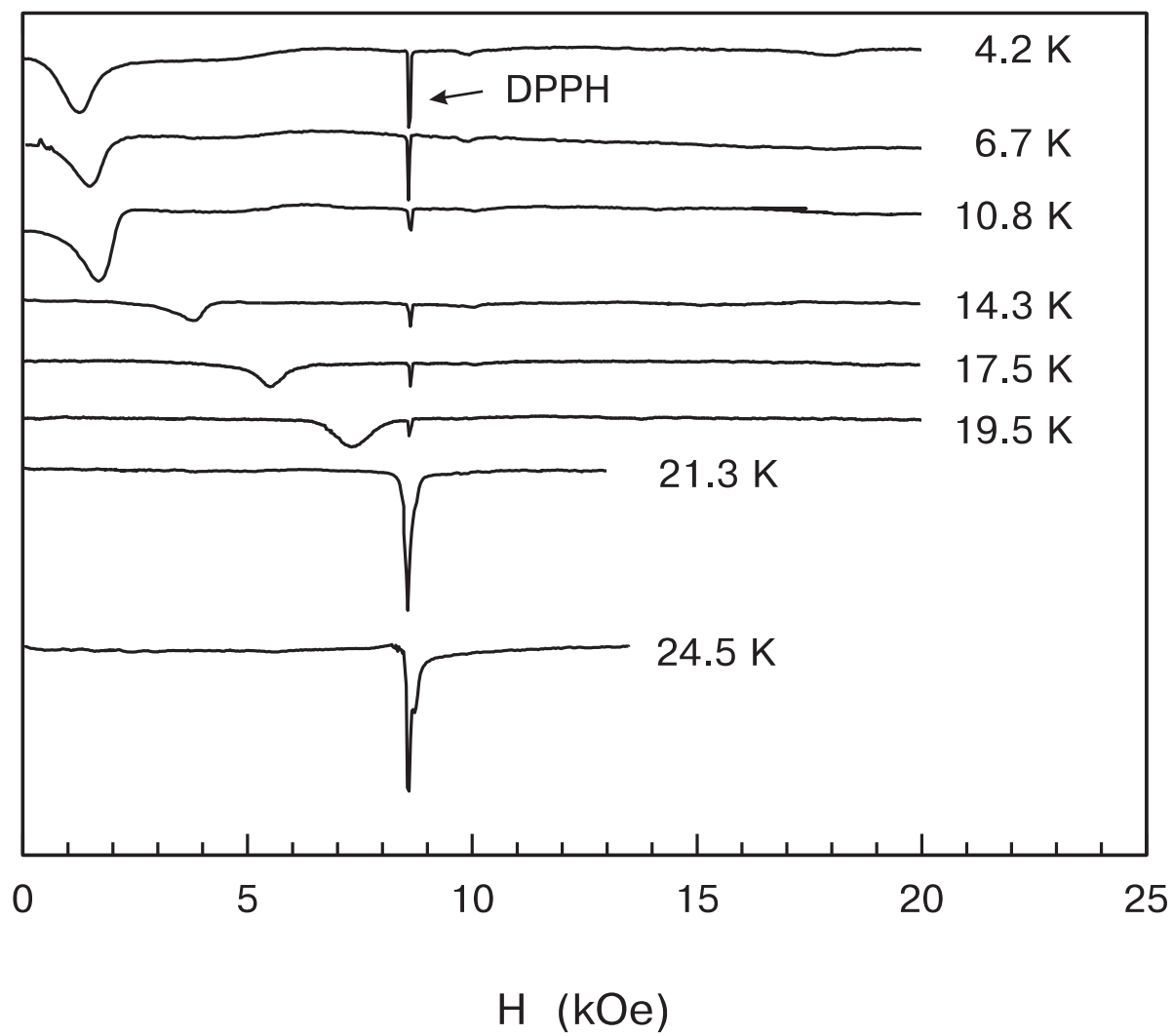


Fig. 4 Vasil'ev et.al.

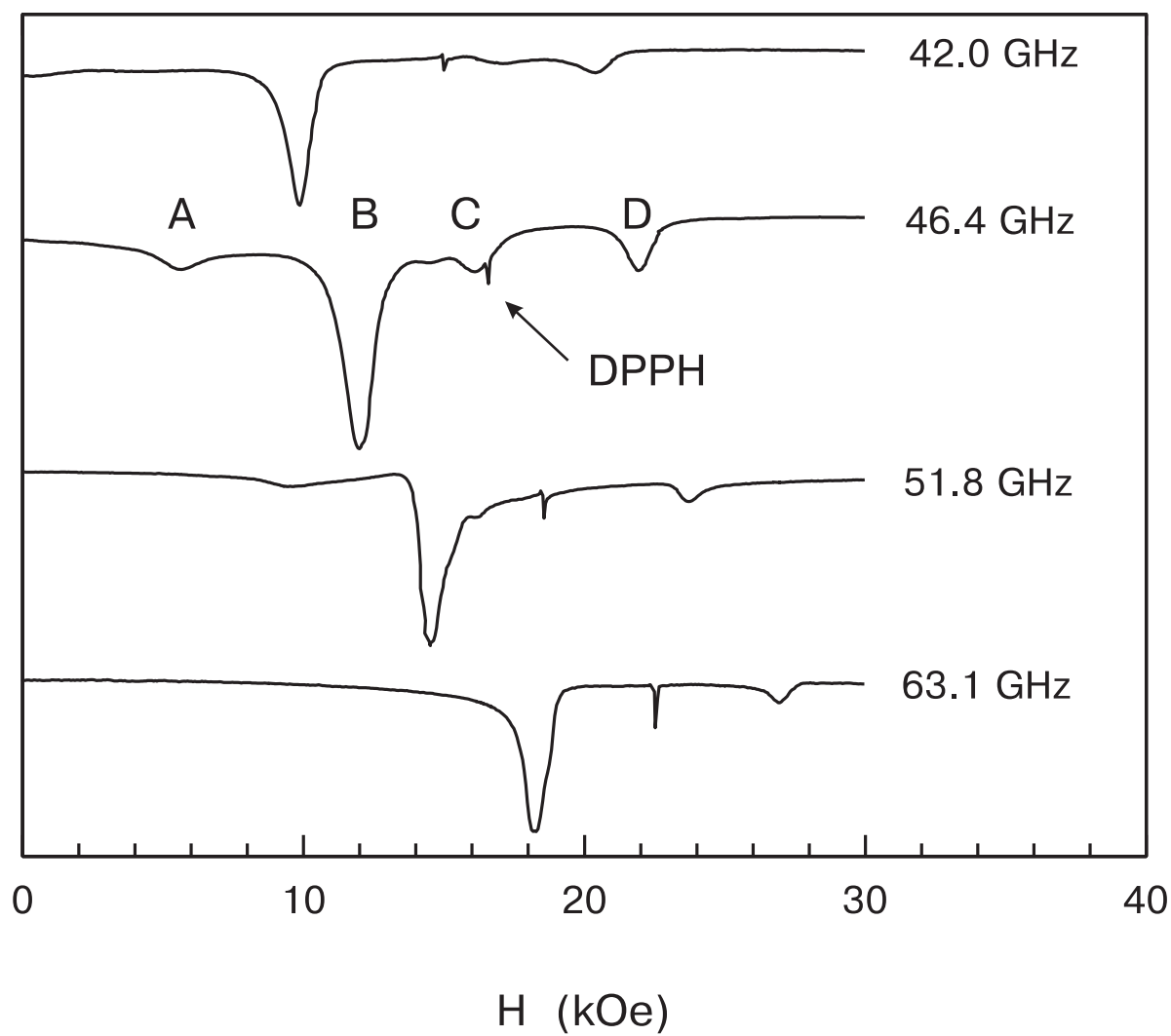


Fig. 5 Vasil'ev et.al.

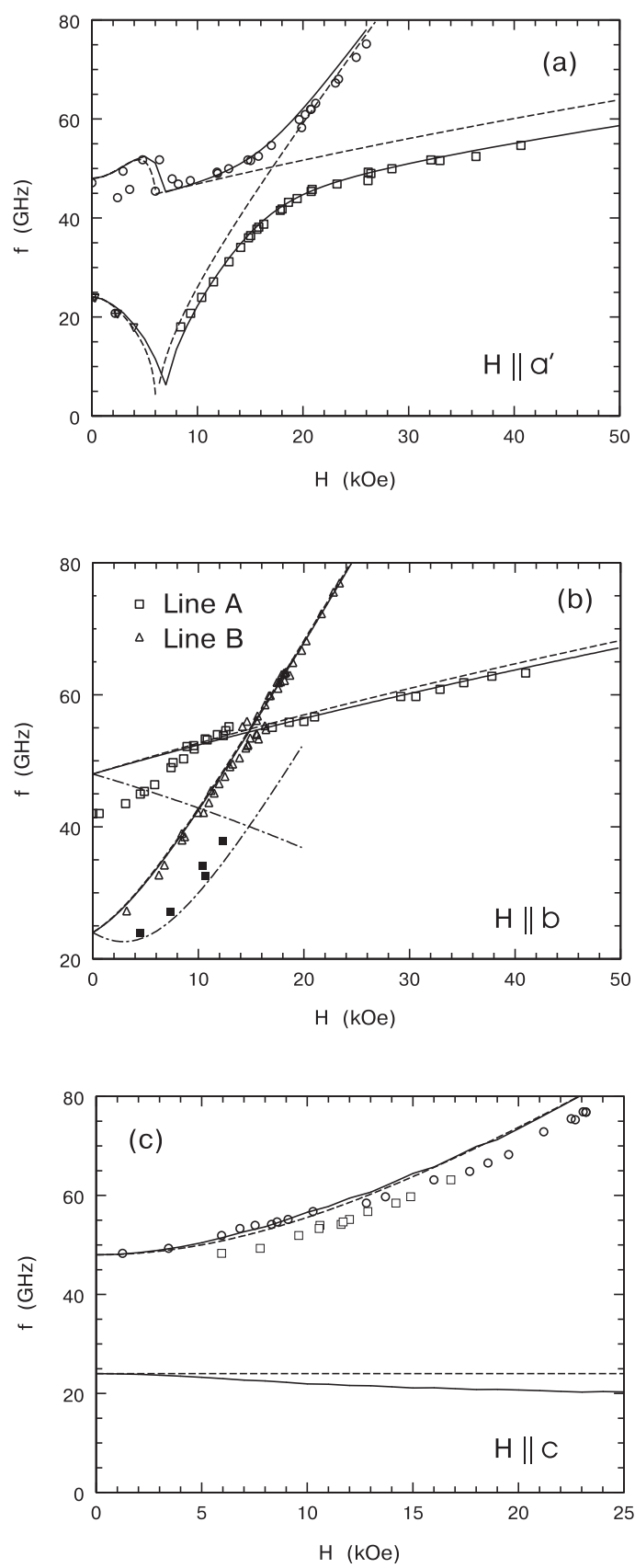


Fig. 6 Vasil'ev et.al.